PHYSICAL REVIEW B VOLUME 24, NUMBER 10 15 NOVEMBER 1981

X-ray-diffraction determination of valence-electron density in aluminum nitride

E. Gabe and Y. Le Page
Division of Chemistry, National Research Council of Canada, Ottawa, KIA OR9 Canada

S. L. Mair
Commonwealth Scientific and Industrial Research Organization Division of Chemical Physics, P. O. Box 160, Clayton, Victoria, 3168 Australia

(Received 30 December 1980)

The valence-electron density in AlN has been measured using x-ray-diffraction intensity data. The effective charge on the nitrogen ion is somewhat dependent on the method of assessment, whether by direct integration of the electron density or by least-squares refinement of a valence population. At $-1.8(\pm 0.8)e$, it falls approximately midway between the ionic and covalent limits. The observed electron density was fitted to a bond-charge model, although clear separation of the bond charge from the valence electrons associated with the nitrogen ion proved not to be possible. In the valence-electron-density contour map the bond charge appears as a small perturbation on the essentially spherical distribution about the anion site. This is in contrast with the case of InSb, where the bond charge is quite conspicuous in the valence-electron-density map.

I. INTRODUCTION

The tetrahedrally coordinated III-V compounds form chemical bonds which are regarded as partially ionic and partially covalent. Such bonds are often characterized by their ionicity, which has a range of zero (fully covalent) to 1 (fully ionic), and by various effective charges which depend very much on the model chosen. Several models of the partially covalent bond have recently been advanced, such as the bond-charge model of Phillips[1] and the bond-orbital model of Harrison.[2]

Recognizing the importance of the valence-electron distribution to our understanding of chemical bonding, Walter and Cohen[3] calculated valence-electron-density maps for several tetrahedrally coordinated semiconductors using an empirical pseudopotential model. More recently, using an improved nonlocal model, the calculations were extended to eleven zinc-blende and diamond structures by Chelikowsky and Cohen.[4] These results reinforce the Phillips bond-charge concept of bonding in that the valence-electron density has as its most prominent feature, an accumulation of electron density between the nearest neighbors displaced towards the more electronegative species. For a homopolar compound this bond charge is at the midpoint of the bond, and in the case of silicon the pseudopotential calculations are in good agreement with the very accurate x-ray diffraction data of Aldred and Hart.[5] X-ray diffraction measurements on heteropolar compounds can provide a clearer understanding of the partially covalent bond and of the status of the bond charge in that situation. Theoretical models of bonding can be assessed by the extent to which they reproduce x-ray diffraction results.

Aluminum nitride is a ceramic material crystallizing in the wurtzite structure (space group $P6_3mc$), which differs from the zinc-blende structure mainly at the relative positions of the third neighbors and beyond.[6] Its valence electrons, being more tightly bound than those of the heavier semiconducting III-V compounds which have been studied previously [e.g., GaAs (Ref. 7), InSb (Ref. 8)], should scatter x rays over a larger range of angles and therefore be more readily observable. Its ionicity on the Phillips scale is 0.445.[1]

With the aim of investigating the valence-electron density in this partially covalent compound, we have measured an extensive, accurate set of x-ray diffraction intensities. The experiment is

described in Sec. II. Our method of analysis, which is set out in Sec. III, is to construct models which give close fits to the data. These provide the phases needed to map out the observed valence-electron density and to integrate over regions around the ions to obtain their electron populations. The models also provide quantitative information on the structural and thermal parameters and the bond charge. In Sec. IV comparisons are made with theoretical predictions and with previous experimental work.

II. DATA COLLECTION AND PRELIMINARY ANALYSIS

Pale green single crystals of AlN, which had been produced by sublimation, were analyzed for impurities. Si was present at an average concentration of 0.15 wt.%, carbon at 0.04 wt.%, and Ni, Cr, Fe, Mn, and Y at less than 0.01 wt.%. One of the crystals was ground to a sphere of 0.36 mm and mounted on a fully automated Picker diffractometer.

Using graphite-monochromated Mo$K\alpha$ x rays ($\lambda_{\alpha_1}=0.70932$ Å), the integrated elastic scattering intensities were measured for 282 reflections and their symmetry-related equivalents, out to $\sin\theta/\lambda=1.22$ Å^{-1}, with the $\theta/2\theta$ scan method, with scan range being increased with θ to allow for wavelength dispersion. Twelve symmetry-equivalent measurements were made for each member of a Friedel pair (hkl and $\bar{h}\,\bar{k}\,\bar{l}$), while the $hk0$ reflections were measured 24 times. The overall agreement between the mean intensities and the individual measurements was 0.80%. Twenty-eight of the measured reflections were of the so-called forbidden type. Rotation about the scattering vector of the lowest-angle quasiforbidden reflections 301, 031, and 331 established that they were too weak to be detected. All forbidden reflections were omitted from the analysis and none of the models described below predicts significant intensities for them.

The integrated intensities were corrected for absorption (using the absorption coefficient,[9] $\mu=11.70$ cm^{-1}) and a Lorentz-polarization factor was applied in which the measured polarization factor of the incident-beam monochromator[10] 0.97 was included. No correction was made for thermal diffuse scattering, as its effect was judged to be minimal in a material with such a high Debye temperature ($\Theta_D=850$ K). Anomalous dispersion corrections for Mo$K\alpha$ radiation were applied and the lattice parameters were taken to be 3.1114 and 4.9792 Å.[11]

The variance $\sigma^2(I)$ associated with the intensity I averaged over symmetry-equivalent measurements, was the sum of the variance from the counting statistics and the estimated variance for the n observed symmetry-equivalent measurements, the latter representing the major source of error. In the subsequent least-squares refinements of the structure factors, the weights w were set to the reciprocal of the variance of the observed structure factors.

The nonlinear least-squares refinements were made using a modified Levenberg-Marquardt algorithm (program ZXSSQ in the IMSL6 subroutine library). Three indicators for the degree of fit to the model were employed:

(i) The goodness of fit (GOF),

$$\mathrm{GOF}=\left[\frac{\sum_{i=1}^{n}\Delta_i^2}{n-m}\right]^{1/2},$$

where $\Delta_i=(F_0-F_c)_i$ is the difference between the ith observed and calculated structure factors, n the number of observations, and m the number of parameters refined.

(ii) The weighted R factor R_w,

$$R_w=\left[\frac{\sum_{i=1}^{n}w_i\Delta^2}{\sum_{i=1}^{n}w_iF_{0_i}^2}\right]^{1/2}.$$

(iii) The R factor R,

$$R=\frac{\sum_{i=1}^{n}|\Delta_i|}{\sum_{i=1}^{n}|F_{0_i}|}.$$

The intense low-angle reflections were severely affected by extinction and a correction had to be applied to bring them up to their kinematic values. Several models for the extinction correction were tried, according to the formulas of Becker and Coppens.[12] The best least-squares fit to the structure factors was obtained with an isotropic secondary extinction correction of type I, with a single parameter g describing the width of the Lorentzian mosaic distribution of crystallites. A highly significant improvement in fit (a drop of 18% in the GOF) was achieved for the same Becker and Cop-

pens type of model, but with an additional parameter representing the fraction f of the total volume of the crystal which was scattering kinematically. This model was proposed by Le Page and Gabe[13] to account for inhomogeneity in the state of perfection of the crystal, such as is produced by grinding at the surface.[14] In this case f was some 25% of the volume (see Table I).

III. VALENCE-ELECTRON-DENSITY MODELS

A. Spherical-ion models

An initial refinement ($R1$) was made using the scattering factors of the isolated neutral atoms. The results are presented in Tables I and II. The structural parameter, $z = 0.38210(6)$, agrees within error with the x-ray diffraction value of Schulz and Thiemann.[15] The thermal parameters of both atomic species are significantly lower than those of Schulz and Thiemann [who obtained $\langle u_{11}^2 \rangle = 0.0037(2)$, $\langle u_{33}^2 \rangle = 0.0040(2)$ for Al, $\langle u_{11}^2 \rangle = 0.0044(2)$, $\langle u_{33}^2 \rangle = 0.0046(4)$ for N, in units of Å^2]. Both analyses revealed very low anisotropies in the thermal motion.

The results of another spherical-ion model ($R2$), in which the population of the valence electrons and the radial expansion or contraction (κ) of the valence shell were varied (as described by Coppens *et al.*[16]) are also shown in Tables I and II. The valence-electron scattering factors used, $f_v(\sin\theta/\lambda)$, were those for the neutral atom[9] normalized to one electron. For example, for nitrogen, $f_v^{\mathrm{N}}(\sin\theta/\lambda)$ was obtained by taking the total scattering factor for the five valence electrons of neutral nitrogen and dividing this by 5. The population of valence electrons associated with nitrogen was then obtained as the multiplier of $f_v^{\mathrm{N}}(\sin\theta/\lambda)$ in the structure-factor expressions, refined subject to the condition of charge neutrality. A significantly improved fit to the observations was obtained with a charge q_{N} of $-1.06(3)e$ on the nitrogen. The refined κ parameters showed contraction of the aluminum valence shell and expansion of the nitrogen shell, consistent with the change in screening from the neutral-atom situation.

The physical meaning of the valence populations refined in this way is not clear cut, especially as the populations are somewhat dependent on the basis functions used. For example, if the Al^{+1} and N^{-1} scattering factors are chosen as a basis,[17] the charge on the nitrogen is increased to $-1.57e$. The populations are therefore critically dependent on the details of the scattering-factor curves in the low-angle region.

An alternative method of estimating the valence populations is to integrate over regions of real space centered on the nuclei. Spherical regions, which are the logical choice for partially ionized species, allow analytical integration of the Fourier series for the electron density (see Kurki-Suonio and Salmo[18]). Then, within a sphere of radius R centered at the origin, the total electron count is

$$Z(R) = \frac{4\pi R^3}{V} \sum_i A_i \frac{j_1(4\pi R \sin\theta/\lambda)}{4\pi R \sin\theta/\lambda} ,$$

where A_i is the real part of the ith structure factor, θ is the scattering angle, λ the x-ray wavelength, and V the volume of the unit cell. The summation may be truncated where the A_i have become negligibly small. If all of the electrons are included in the integration, the series extends out to $\sin\theta/\lambda$ values far beyond the limit available with Mo $K\alpha$ radiation, but if only the valence electrons are counted, the scattering is confined to the lower an-

TABLE I. Structural, thermal, and extinction parameters for refinements $R1$,$R2$,$R3$. The figures in parentheses are the estimated standard deviations of the parameters.

Refinement	S[a]	z	$\langle u_{11}^2 \rangle$ Al (Å$^2\times10^4$)	$\langle u_{33}^2 \rangle$ Al (Å$^2\times10^4$)	$\langle u_{11}^2 \rangle$ N (Å$^2\times10^4$)	$\langle u_{33}^2 \rangle$ N (Å$^2\times10^4$)	g	f
$R1$	38.92	0.382 10	32.1	32.9	38.7	40.1	3525	0.251
	(0.05)	(0.000 06)	(0.3)	(0.3)	(0.5)	(0.6)	(52)	(0.003)
$R2$	38.84	0.382 01	31.6	33.1	39.7	39.4	3072	0.207
	(0.04)	(0.000 05)	(0.2)	(0.3)	(0.4)	(0.5)	(35)	(0.002)
$R3$	39.06	0.382 01	31.8	33.4	39.5	38.2	3387	0.197
	(0.04)	(0.000 04)	(0.2)	(0.2)	(0.4)	(0.5)	(32)	(0.002)

[a]S is a scale factor to take account of the incident-beam intensity.

TABLE II. Population and bond-charge parameters and agreement factors for refinements $R1$,$R2$,$R3$. The figures in parentheses are the estimated standard deviations of the parameters.

Refinement	q_N (electrons)	κ_N	κ_{Al}	P_{bond} (electrons)	B_{bond} (Å^2)	x[a]	R	wR	GOF
$R1$	0.0	1.0	1.0	0.0			1.21	0.91	1.08
$R2$	−1.06	0.913	1.069	0.0			1.10	0.70	0.83
	(0.03)	(0.004)	(0.012)						
$R3$	−1.89	1.0	1.0	0.71	17.1	0.689	0.98	0.62	0.74
	(0.01)			(0.07)	(0.2)	(0.003)			

[a]Fractional distance of bond-charge center along the bond from the Al site.

gles and the truncation effect is negligible.

In assigning a population Z there is a degree of arbitrariness in the choice of radius R. Kurki-Suonio and Salmo[18] have suggested that the radius should be chosen at the minimum in $4\pi r^2\rho(r)$, where

$$\rho(r)=\frac{1}{V}\sum_i A_i\frac{\sin(4\pi r\sin\theta/\lambda)}{4\pi\sin\theta/\lambda}$$

is the radial electron density centered on the origin.

Figures 1(a) and 1(b) show the observed $4\pi r^2\rho(r)$ and $Z(r)$ for Al and N, respectively, in AlN, with phases assigned according to R2 (Table I). Also shown are the calculated curves for a model crystal built from isolated neutral atoms and from isolated monovalent ions, and, in Fig. 1(c), the calculated core scattering. The core scattering has been calculated out to $\sin\theta/\lambda=12$ Å^{-1}, using a one-dimensional cell of 50 Å (see James [19]).

The Al curves [Fig. 1(a)] show little difference in electron count for Al^{+1}, Al^0, and the observed Al. The minimum in $4\pi r^2\rho(r)$ is at approximately 1.15 Å for all curves, defining a Z of 2.9e. Similar insensitivity of $4\pi r^2\rho(r)$ and $Z(r)$ to the valence of the free model atoms has been observed[18] in the alkali halides and may be attributed to the overlapping of electron density on forming the crystal.

The observed nitrogen curves are more reliable than the Al ones because there are more nitrogen valence electrons to act as scatterers for the x rays and the scattering extends out to higher angles. The N curves show a clearer difference between the observed and model atom results. Above 0.9 Å the observed Z values are higher than those for N^0 and N^-, suggesting that the nitrogen has a charge more negative than −1 electron. The observed $4\pi r^2\rho(r)$ curve is more diffuse than the model curves, with a minimum at a higher radius (1.52 Å), corresponding to $Z=7.4e$ (i.e., a charge of $-2.4e$).

The core scattering [Fig. 1(c)] is all contained within a radius of 1 Å. This is smaller than the radii of the spheres of integration for the valence electrons, so that the core scattering does not affect the $Z(R)$ for the valence electrons.

The error in $Z(R)$ and $4\pi r^2\rho(r)$ due to the error in the real part of the structure factors A would be barely discernible on the scale of Figs. 1. The major source of error is in the assignment of phase to the observed structure factors. To give some idea of the size of this error, the curves of Fig. 1(b) for nitrogen were recalculated with phases from the initial refinement ($R1$). The resulting $Z(R)$ was reduced to 6.2e. However, for the final, aspherical model $R3$ described below, $Z(R)$ remained unchanged at 7.4e.

Although it is obvious that the valence (i.e., the charge associated with each species) of AlN cannot be defined very closely, it is clear that the charge on the nitrogen lies somewhere within the limits −1 to −2.5 electrons. It is probably not realistic to give a more exact value in a partially covalent compound, as this involves making arbitrary definitions about the boundaries of the atom.

B. Nonspherical-ion models

It might be expected that the covalency in AlN would be associated with an asphericity in the valence-electron density. The difference electron density for $R2$ (Fig. 2) (i.e., the remaining electron density calculated from the difference between the observed structure factors and the model ones) does not show any of the expected buildup of electron density in the bonds. However, in a noncentrosymmetric structure, the difference map minimizes the

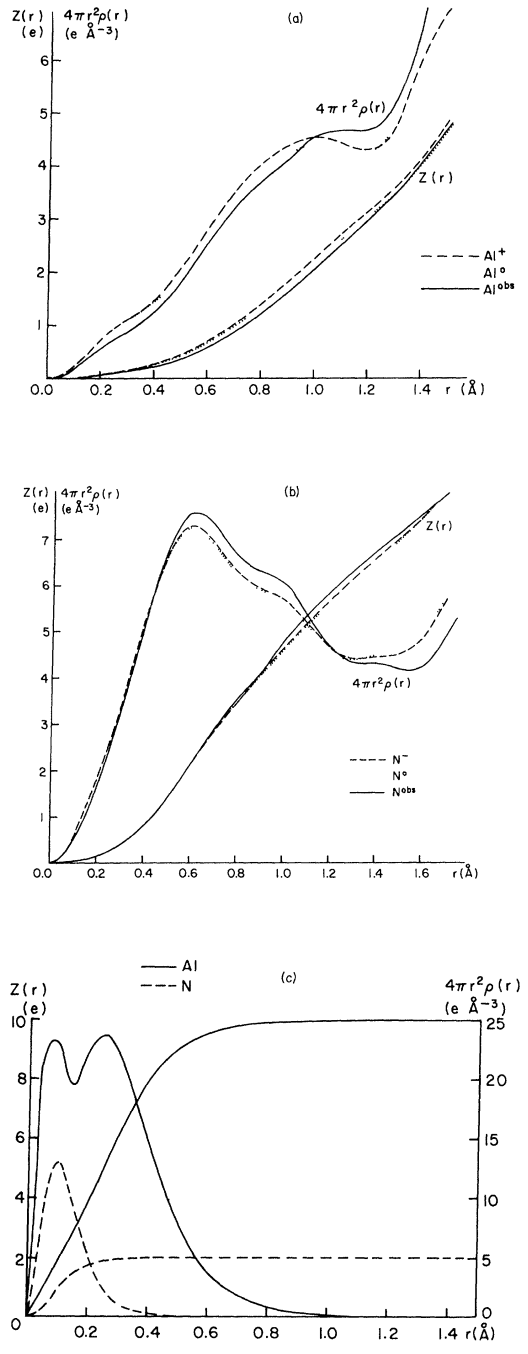

FIG. 1. Electron count $Z(r)$ in a sphere of radius r and $4\pi r^2\rho(r)$, where $\rho(r)$ is the radial electron density (a) for valence electrons of Al in AlN [theoretical curves for a model in which Al is (i) the isolated neutral atom and (ii) the monovalent cation, are also shown], (b) for valence electrons of N in AlN (theoretical curves for N and N^- are also shown), (c) calculated for the Al and N cores.

remaining electron density, since the phases are assumed to be those of the model. Nonspherical effects could not, therefore, be ruled out at this stage, although it was clear that, if present, they would be small. A model was required which would allow for some extra electrons in the bonds, presumably nearer to the more electronegative species, i.e., the nitrogens. A full multipole model[20] was ruled out because it would require too many extra parameters, viz., the population and exponent for a dipole, a quadrupole, and two octupoles for each species. (Although there are 282 independent reflections, only 34 of these are in the low-angle region, $\sin\theta/\lambda$ less than 0.55 $Å^{-1}$, where the valence electrons contribute significantly.) A limited mulitpole model, which retained only the two octupoles, did not provide a significantly better fit to the data.

An alternative model ($R3$), requiring one more parameter than model $R2$, was more successful. This was a bond-charge model, in which an isotropic Gaussian distribution of electron density was placed in the bond. The charge-transfer parameter q_N of model $R2$ was retained, but the two valence-shell expansion parameters κ were dropped to avoid overparametrization. The bond-charge parameters were its population P_{bond} (which was constrained to maintain crystal neutrality), the Gaussian spread parameter B_{bond} (which was treated, in effect, like a harmonic Debye-Waller factor), and the fractional distance x of the bond-charge center along the bond from the Al atom. The bond-charge scattering factor is then

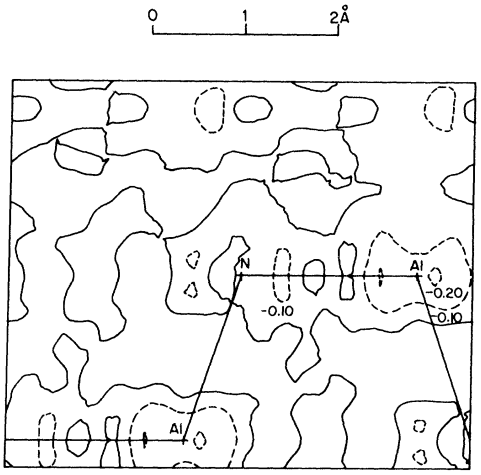

FIG. 2. Difference electron density in the (110) plane for model $R2$. Full contours are at zero $0e$ $Å^{-3}$.

$$P_{\text{bond}}\exp(-B_{\text{bond}}\sin^2\theta/\lambda) .$$

A similar model has been used recently to describe the bonding in silicon.[21] Although the multipole model is perhaps preferable in the highly symmetric diamond structures,[22] the bond-charge model has advantages when a lower symmetry increases the number of possible multipoles.

The results of $R3$ are presented in Tables I and II. Judged by the 12% decrease in the GOF below that of model $R2$, the bond-charge model is significantly better. This conclusion is supported by the R-factor test of Hamilton,[23] which assigns model $R3$ a significance level of 0.005 (i.e., there is 0.5% probability of error if the hypothesis that the ions are spherical is rejected).

The refined bond charge is $0.7e$, located 69% of the bond-length away from Al, with Gaussian spread parameter of 17 Å^2. If all of the four bond charges are associated with the nitrogen, the refined charge on that atom q_N becomes $-1.9e$. As a small proportion of the bond charge should be allotted in some way to the aluminum, this value of q_N represents a lower bound for the $R3$ model.

The values shown in parentheses in Tables I and II represent the estimated standard deviations (e.s.d.'s) of the parameters, but for the bonding parameters they are not a true estimate of the total error, as these parameters are dependent on an extinction model which necessarily relies on certain simplifying assumptions. These include the treatment of the multiple scattering by intensity coupling (incoherent scattering) rather than as a coherent-scattering problem, and the assumption of a homogeneous distribution of imperfections throughout the volume of the crystal exhibiting extinction.

The valence-electron density for $R3$ is shown in Fig. 3. The effect of the bond charge is a very small perturbation on the spherical distribution of electron density centered on the nitrogen species. Figure 4(a) shows the difference electron density when the calculated spherical charges of model $R3$ are subtracted from the observed electron density. The asphericity about the nitrogen in this map has been modeled in terms of the bond charges.

Figure 4(b) shows the profile along the bond axis of a single bond charge. The position of the nitrogen nucleus is marked with an arrow. The superposition of the four bond charges will produce a maximum electron density at the nitrogen position, as observed in Fig. 4(a). For this reason the bond charge cannot be interpreted literally as a charge wholly associated with the bond.

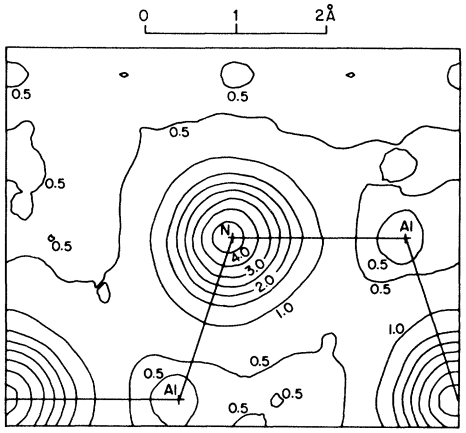

FIG. 3. Observed valence-electron density in the (110) plane of AlN. Contours are at $0.5e$ Å^{-3} intervals.

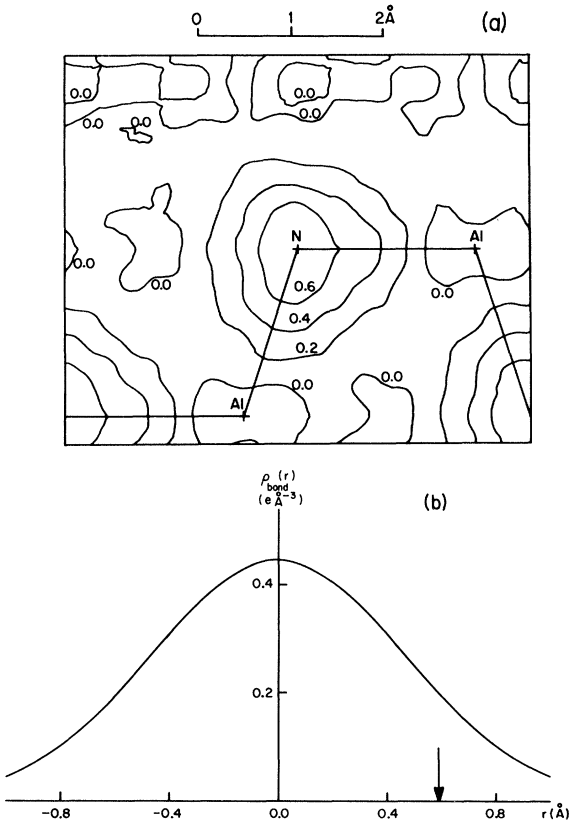

FIG. 4. (a) Difference electron density in which the calculated spherical component at the atom sites, according to model $R3$, has been subtracted from the observed electron density in the (110) plane of AlN, with contour intervals at $0.2e$ Å^{-1}. (b) The electron density for a single bond charge, according to model $R3$, shown as a profile along the bond axis. The position of the nitrogen nucleus, marked with an arrow, is the same for all four bonds within the scale of the diagram.

IV. COMPARISON WITH PREVIOUS WORK

Schulz and Thiemann[15] carried out a refinement for the charge on the nitrogen in AlN. They used scattering factors obtained by extrapolation from the N^0 and N^{-1} curves. No radial expansion parameters were refined. They obtained a charge of $-1.66(0.50)e$, which is in agreement, within error, with the values obtained here in the various refinements, but somewhat lower than that from the electron-density integration technique. A slightly lower value is predicted by the bond-orbital model of Harrison,[2] using the effective-charge parameter (multiplied by -1). The result of $-1.29e$ is closest to the value ($-1.06e$) obtained in the $R2$ refinement.

Further evidence for electron transfer in AlN is available from preliminary x-ray photoelectron spectroscopy measurements (Dr. R. Leckey and Dr. J. Liesegang, private communication). Changes in the binding energy of the inner electron shells from the isolated atom values are consistent with some transfer of electrons from the Al to the N on formation of AlN.

The material most closely related to AlN and for which accurate valence-electron data are available is InSb.[8] This is a III-V semiconductor which crystallizes in the cubic ZnS structure. Since the authors did not use a bond-charge model to analyze their data on InSb, a reanalysis has been carried out[24] using an $R3$-type model. The valence-electron density calculated for this model (Fig. 5) is in qualitative agreement with the pseudopotential calculations of Chelikowsky and Cohen.[4] The bond peaks are of similar magnitude, although at both the Sb and In sites the pseudopotential electron densities are some $0.1e$ Å^{-3} lower than those from the $R3$-type model of the data.

The bond-charge parameters and ionicities[1] are compared for InSb, AlN, and Si (Ref. 21) in Table III. Allowing for a significant nitrogen-centered component in the bond charge for AlN, the bond-charge parameters reflect the expected trend with ionicity.

The appearance of the valence-electron-density in AlN (Fig. 3) is quite different from that of InSb (Fig. 5), where the dominant feature is the bond charge itself. In AlN the dominant feature is the nearly spherical distribution of electrons about the nitrogen ion.

V. CONCLUSIONS

Our investigations of AlN have shown that it conforms in some respects to accepted ideas of tetrahedrally coordinated, partially covalent compounds. It has a valence of some $1.8(\pm 0.8)e$, that is, in the middle range between the covalent and ionic limits (in this case 0 and $3e$, respectively), and in fair agreement with the prediction of the bond-orbital model.[2] Its bond charge is not clearly separable from the nitrogen ion valence density, but appears to be consistent with its ionicity when

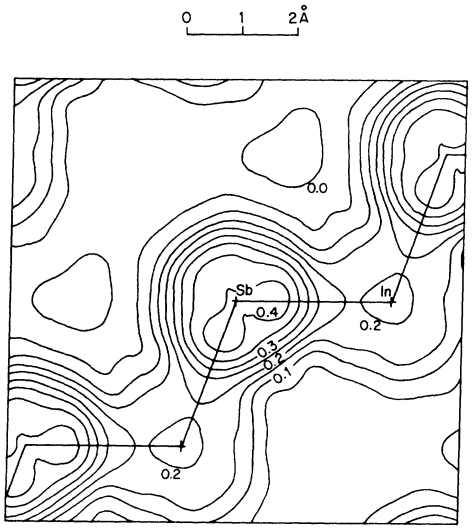

FIG. 5. Calculated valence-electron density for InSb in the (110) plane, according to the bond-charge model with parameters as shown in Table III. Contours are at $0.5e$ Å^{-3} intervals.

TABLE III. Comparison of bond charges for AlN, InSb, and Si. For InSb and Si the values in parentheses are estimated standard deviations. For AlN the bond-charge parameters should be treated as rough estimates of the bond charge itself, as they include an unspecified nitrogen-centered component. Accordingly, P_{bond} represents an upper limit for the bond-charge population.

	AlN	InSb (Refs. 8,24)	Si (Ref. 21)
$P_{\text{bond}}(e)$	0.7	0.3 (0.1)	0.56 (0.06)
B_{bond}(Å^2)	17	21 (4)	22[a] (1)
x[b]	0.69	0.69 (0.01)	0.50
Phillips ionicity (Ref. 1)	0.445	0.321	0.0

[a]Isotopic average. [b]Fractional distance of bond-charge center along bond from site of Al, In, or Si.

compared with InSb and Si.

It is only in the appearance of the valence-electron density in AlN that the traditional idea of a cloud of bonding electron density has to be modified. The bond-cloud concept is, to some extent, preserved in the III-V semiconductors as calculated from empirical pseudopotentials[4] and from experimental work on Si (Refs. 5,21) and InSb (Ref. 8), but in AlN the valence electrons are only slightly perturbed from spherical distributions on the ion sites. This is a consequence of the greater localization of electrons in the low-Z species, resulting in a higher peak intensity at the anion site and very poor resolution of the bond charge itself.

The present electron-density analysis has illustrated some of the problems of interpreting diffraction measurements from noncentrosymmetric structures. The indeterminacy in the phases means that details in the electron density, although they be larger than the experimental error, may only become obvious after their existence is recognized through inclusion in a trial model for the structure factors.

ACKNOWLEDGMENTS

We wish to thank Dr. A. McL. Mathieson for his continued interest in this work and the resulting useful discussions. We are indebted to Mr. A. F. Armington, of the U. S. Department of the Air Force for providing us with the sample, to Broken Hill Pty, Ltd. Melbourne Research Laboratories for its composition analysis, and to Dr. J. Tibballs for help in preparation of the spherical specimen.

[1]J. C. Phillips, Rev. Mod. Phys. 42, 317 (1970).
[2]W. A. Harrison, Phys. Rev. B 8, 4487 (1973).
[3]J. P. Walter and M. L. Cohen, Phys. Rev. B 6, 1877 (1971).
[4]J. R. Chelikowsky and M. L. Cohen, Phys. Rev. B 14, 556 (1976).
[5]P. J. E. Aldred and M. Hart, Proc. R. Soc. London Ser. A 332, 223 (1973); Y. W. Yang and P. Coppens, Solid State Commun. 15, 1555 (1974).
[6]P. Lawaetz, Phys. Rev. B 10, 4039 (1972).
[7]R. Uno, T. Okano, and K. Yukino, J. Phys. Soc. Jpn. 28, 437 (1970).
[8]D. H. Bilderback and R. Colella, Phys. Rev. B 13, 2479 (1976).
[9]*International Tables for X-ray Crystallography* (Birmingham, Kynoch, 1974), Vol. IV.
[10]Y. Le Page, E. J. Gabe, and L. D. Calvert, J. Appl. Crystallogr. 12, 25 (1979).
[11]Natl. Bur. Stand. Monogr. 25, Sec. 12 (1974).
[12]P. Becker and P. Coppens, Acta Crystallogr. Sect. A 30, 129 (1974).
[13]Y. Le Page and E. J. Gabe, J. Appl. Crystallogr. 11, 254 (1975).
[14]J. M. Boehm, P. R. Prager, and Z. Barnea, Acta Crystallogr. Sect. A 30, 335 (1974).
[15]H. Schulz and K. H. Thiemann, Solid State Commun. 23, 815 (1977).
[16]P. Coppens, T. N. Guru Row, P. Leung, E. D. Stevens, P. J. Becker, and Y. W. Yang, Acta Crystallogr. Sect. A 35, 63 (1979).
[17]T. Fukamachi, Tech. Rep. Inst. Solid State Phys. Univ. of Tokyo Ser. B 12, 1 (1971).
[18]K. Kurki-Suonio and P. Salmo, Ann. Acad. Sci. Fenn. Ser. A VI, 369, 1 (1971).
[19]R. W. James, *The Optical Principles of the Diffraction of X-rays* (Bell, London, 1954), p. 408.
[20]R. F. Stewart, Acta Crystallogr. Sect. A 32, 565 (1976).
[21]C. Scheringer, Acta Crystallogr. Sect. A 36, 205 (1980).
[22]B. Dawson, Proc. R. Soc. London Ser. A 298, 264 (1967). P. F. Price, E. N. Maslen, and S. L. Mair, Acta Crystallogr. Sect. A 34, 183 (1978).
[23]W. C. Hamilton, Acta Crystallogr. 18, 502 (1965).
[24]S. L. Mair, unpublished.